Electronic Supplementary Information:

Tuning local microstructure of colloidal gels by ultrasound-activated deformable inclusions

Brice Saint-Michel, George Petekidis and Valeria Garbin

Contents

1 Gel rheology

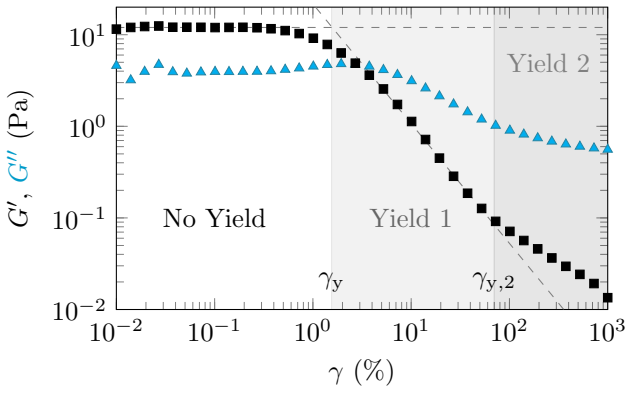

SI Figure 1 Amplitude Sweep of the colloidal gel under study for an angular frequency of 1 rad.s^{-1}.

The rheology of the gel shown in Figure 1 has been measured using an Anton Paar MCR 501 rheometer working in oscillatory mode, performing an amplitude sweep at $f = 1$ Hz.

2 Effect of ultrasound in the absence of bubbles

SI Figure 2 shows the effect of the application of ultrasound pulses away from the geometry boundaries when no bubbles are present. We apply pulses close to the maximum transducer voltage ($U \geq 200$ V peak-to-peak), a large number of cycles $N = 10000$ and several frequencies ($f = 15$ kHz, $f = 20$ kHz, $f = 10$ kHz successively), i.e. a pulse intensity and duration exceeding what is applied in the main text.

The initial pulses at 15 kHz have little impact on the gel aside from a small drift, as the same features may be seen in SI Figure (a) and (b). SI Figure (c) shows that applying the 20 kHz pulse produces an apparently new, yet similar microstructure, whereas the initial microstructure is recovered after applying the 10 kHz pulse. Hence, applying ultrasound without bubbles does not affect the gel microstructure but may induce a small displacement of our experimental chip with respect to the microscope.

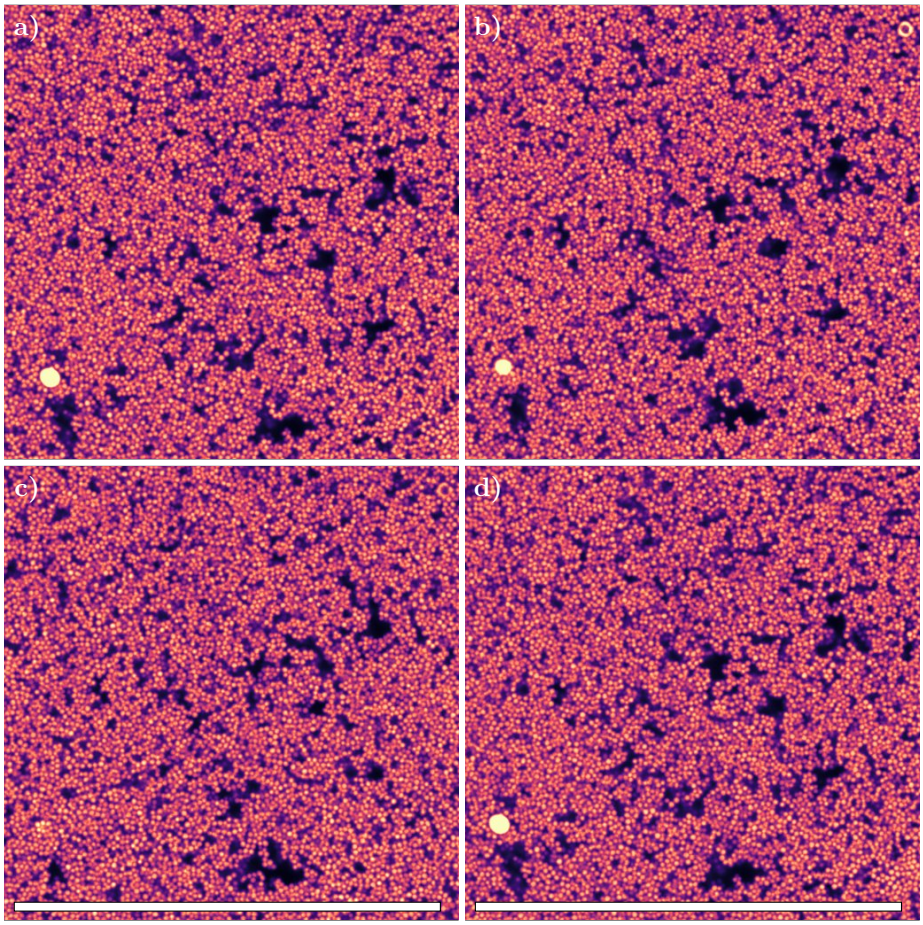

SI Figure 2 Effect of ultrasound pulses on the gel when no bubbles are present. a) Initial state. b) Gel after 15 kHz pulses have been applied. c) Gel after 20 kHz have been applied. d) Gel after the 10 kHz pulses have been applied. The scale bars are 100 μm

3 Particle detection

The quality of the particle detection routines we use can be assessed in Figure 3. We observe that the proximity of the bubble results in a locally darker picture and several missed particles, whereas particles are accurately detected further away from it. Some of the detected particles appear darker than others as they are not perfectly in the field of view of the confocal slice.

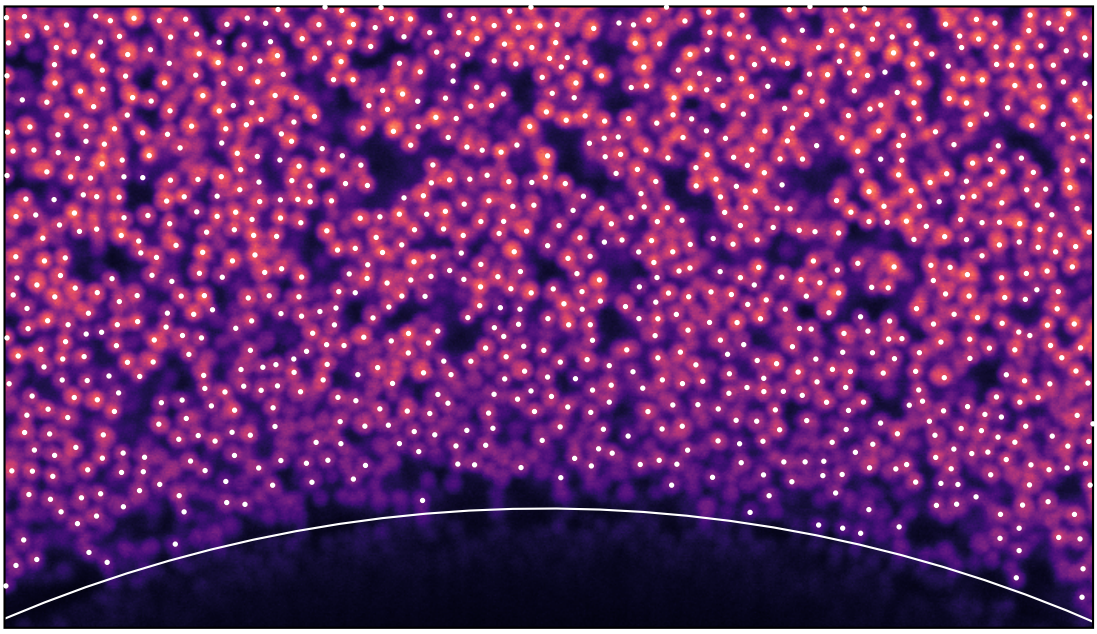

SI Figure 3 Close-up of a confocal image of the colloidal gel around a bubble. Small white dots indicate detected particles. The white solid line shows the detected bubble radius. The picture width is 70 μm.

4 Confocal videos of bubble dissolution

`SI_Video1` shows a confocal acquisition of the bubble dissolving presented in Figures 2 and 3. The picture size is 300 μm $\times$ 300 μm, i.e. with a larger field of view than Figure 2, and frames are recorded every 12 s. Complete bubble dissolution is achieved around 1000 s.

5 Impact of bubble dissolution and acoustic excitation on the local volume fraction

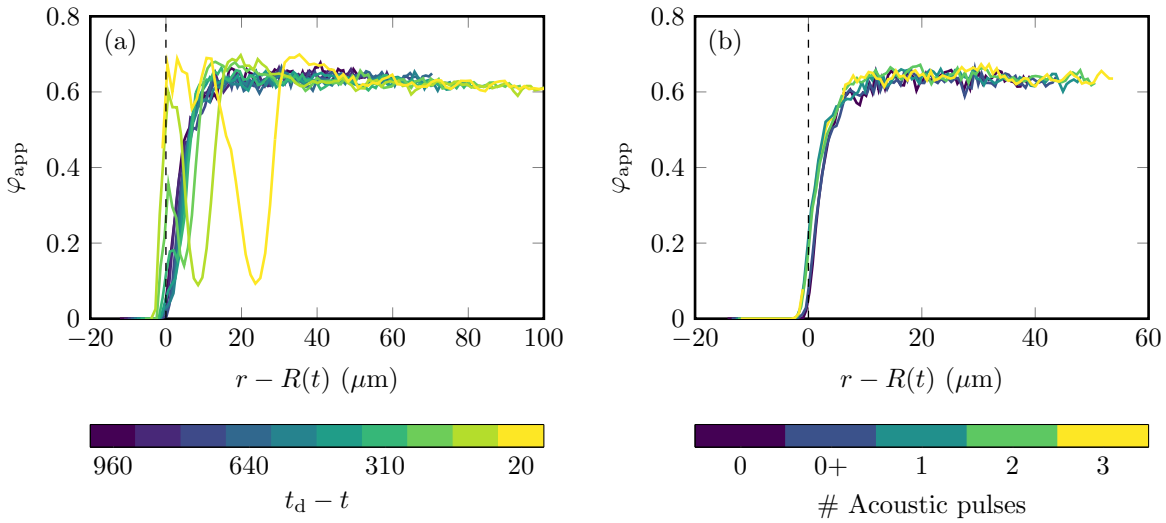

SI Figure 4 Estimated surface fraction φ_{app} close to the bubble edge during (a) a bubble dissolution experiment and (b) a bubble oscillation experiment. The origin of the x axis corresponds to the detected bubble edge. The color bars code for the time before dissolution in (a) and the number of applied ultrasound pulses in (b). The $0+$ label corresponds to the application of a small pulse, insufficient to rearrange the gel, while particle rearrangement is noticeable after pulses 1,2 and 3.

SI Figure 4 details how the (estimated) particle fraction φ_{app} evolves with time close to the bubble during both dissolution and oscillation experiments. This quantity is based on the detected particle positions and the typical area of a particle πa^2. Other indicators (e.g. local fluorescence intensity) provide similar results.

During bubble dissolution [SI Figure 4(a)], we observe a marked minimum of φ_{app} growing with time for small, positive $r-R(t)$. This minimum corresponds to the solvent pocket. At later times, we also notice a slight increase of φ_{app} just beyond the solvent pocket, as also noted in fibrillated cellulose gels[1]

During bubble oscillation experiments [SI Figure 4(b)], we note that the application of ultrasound pulses and the subsequent particle rearranging does not impact the local volume fraction.

6 Real-time brightfield microstreaming observations

The video entitled `SI_Video2` show videos a bubble taken with the real-time brightfield setup, corresponding to the microstreaming snapshots taken in Figure 6 of the main text. The bubble has a radius $R = 167$ μm at rest and assumes a squeezed, pancake shape. The bubble interface becomes blurry when the ultrasound excitation is applied ; we vary its intensity before stopping it during the video. Our main observation is that microstreaming is visible, yet slower for smaller acoustic excitation and bubble oscillations. Microstreaming stops immediately, or at least lasts less than one inter-frame (0.22 s) when the acoustic excitation is stopped.

7 Time-aliased brightfield oscillations and microstreaming

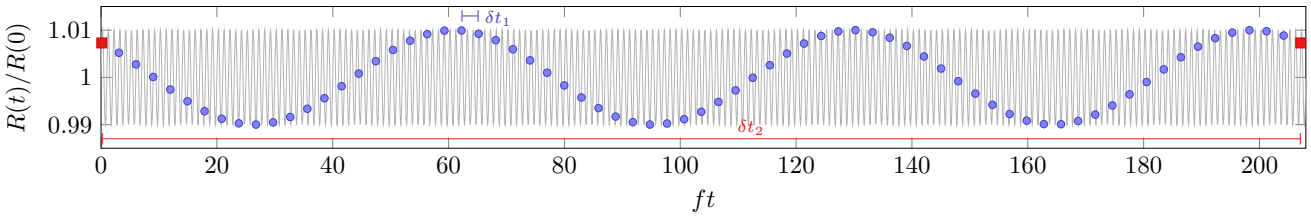

SI Figure 5 Time aliasing during high-speed imaging of ultrasound bubble oscillations. The grey line represents the bubble radius, while the blue circles denote the time at which each high-speed frame is captured. They are separated by a time $\delta t_1 = 1/7000$ s $= 1.43 \times 10^{-4}$ s. Every 70 frames (corresponding to 207 oscillation cycles and to δt_2), the camera records the same "instant" of a (different) oscillation cycle, allowing true stroboscopic acquisitions. A pair of 'stroboscopic' frames is shown as red squares.

ESI Figure 5 shows how the aliased image acquisition works. The sampling rate of our camera $1/\delta t_1 = 7000\ \mathrm{s}^{-1}$ does not allow to resolve one oscillation cycle, but using a very short exposure time ($1/148\,000$ s) allows us to obtain sharp images of the bubble. Using this "low" sampling rate allows us to acquire frames with the full camera resolution, i.e. 1024×1024 pixels. We actually choose δt_1 to be close to a multiple of $1/f$, the inverse of the oscillation frequency $f = 20.7$ kHz:

$$f\delta t_1 = k - \delta \quad \text{with} \quad k = 3 \quad \text{and} \quad \delta = \frac{3}{70}. \tag{1}$$

At steady state, for which successive bubble oscillation cycles are identical, we are then probing different "instants" of the oscillation cycle with a good effective sampling rate since $0 < \delta \ll 1$. This technique is called *intentional time aliasing*, intentional undersampling or bandpass sampling[2]. In addition, every $P = 70$ frames, $Pf\delta t_1$ is an integer, which means the bubble oscillation "instants" separated by $\delta t_2 = P\delta t_1$ precisely coincide. These pairs of frames are true stroboscopic acquisitions of the oscillations separated by $N = Pf\delta_1 = 207$ oscillation cycles. We can then both estimate the bubble oscillation amplitude and the microstreaming even when our acquisition is not strictly time-resolved.

The time aliased videos `SI_video3` and `SI_video4` follow this procedure. `SI_Video3` is taken at $1/\delta_1 = 7000$ frames per second and allows us to determine the bubble oscillation amplitude by looking at the maximum and minimum bubble radius over a period exceeding $P = 70$ frames, from which we obtain $x = 0.03$. `SI_Video4` takes one every seventy images of `SI_Video3` to perform true stroboscopy and highlight microstreaming.

Notes and references

1 J. Song, M. Caggioni, T. M. Squires, J. F. Gilchrist, S. W. Prescott and P. T. Spicer, Rheol. Acta **58**, 231-239 (2019)

2 R. G. Vaughan, N. L. Scott and D. R. White, IEEE Trans. Signal Process. **39**(9), 1973-1984 (1991)